

Curvature Blindness from Polarity Breaks and Orientation Channel Fragmentation in V1

Michael Menke

Abstract

We present a mathematical model of the curvature blindness illusion in which sinusoids appear as angular zigzags when drawn with alternating contrast polarity against a gray background.

The model identifies two complementary mechanisms, both operating in V1. First, *polarity channel separation*: simple cells are selective for contrast polarity, and lateral connections link only same polarity neurons; where the line switches from darker than background to lighter than background at each peak and trough, the encoding population changes and the lateral chain is broken, segmenting the contour into half-wavelength pieces. Second, *orientation channel fragmentation*: at moderate contrast, the active orientation window is narrow, and within each half-wavelength segment no single orientation channel spans the full range of edge normals; the inflection point at the center of each segment anchors a locally straight percept. Together, the two mechanisms produce a zigzag: polarity breaks supply the corners, and fragmentation straightens the segments between them.

The model yields three necessary conditions for the illusion: (i) the curve must have contrast polarity reversals (to create segment boundaries); (ii) the contrast must be moderate (to narrow orientation channels); and (iii) the curve must have inflection points between successive polarity reversals (to provide locally straight anchors). Condition (iii) predicts that the illusion should generalize to any polarity alternating curve with sign-changing curvature (S-curves, damped oscillations).

1 Introduction

1.1 The illusion

The curvature blindness illusion, discovered by Takahashi [11], is a failure of curvature perception. In the standard stimulus, a sinusoidal line is drawn against a gray background with its luminance alternating between darker than background and lighter than background, the switch occurring at each peak and trough. The line appears to have sharp corners at its peaks and troughs, as if it were a zigzag. The same line is correctly perceived as smooth at high contrast against a white or black background [11]. The illusion requires that amplitude cannot be too large: large amplitude sinusoids are perceived as curved even on a gray background [11]. Bertamini and Kitaoka [2] suggested informally that corner detecting mechanisms may be responsible, but did not provide equations or testable conditions.

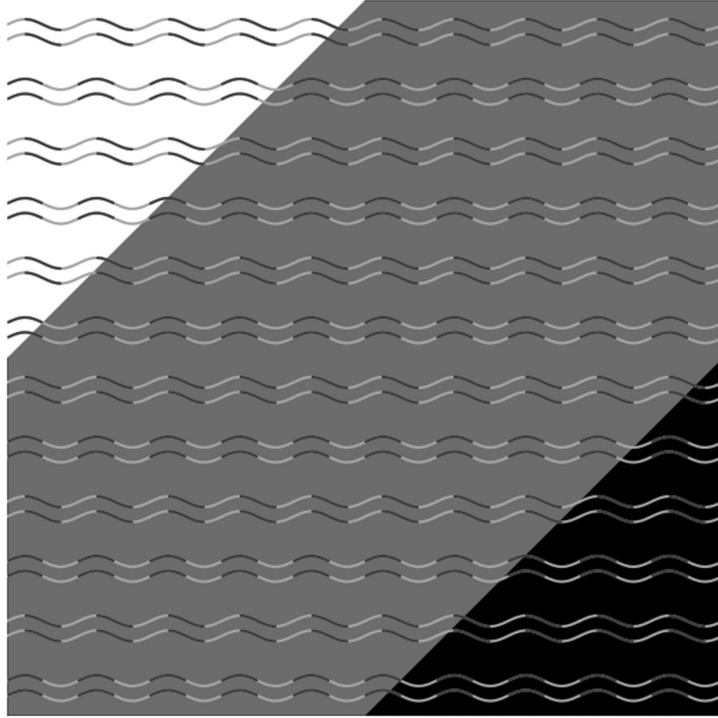


Figure 1: The curvature blindness illusion (from Takahashi [11]). Sinusoidal curves with alternating dark/light segments appear smooth against the white and black backgrounds, but appear as angular zigzags against the gray background.

1.2 The main ideas

We identify two V1 mechanisms that jointly produce the illusion.

Polarity channel separation. V1 simple cells are selective for contrast polarity: a cell that responds to a dark to light edge does not respond to a light to dark edge at the same orientation [7]. Lateral connections in V1 preferentially link neurons of matched polarity as well as matched orientation [3, 5]. Where the stimulus line switches from darker than background to lighter than background, the encoding population changes entirely, and the lateral chain that mediates contour integration is broken. In the Takahashi stimulus, these polarity switches occur precisely at the peaks and troughs of the sinusoid, segmenting the contour into half wavelength pieces.

Orientation channel fragmentation. Perceiving curvature within a segment requires comparing edge orientations across nearby positions, via lateral connections linking neurons with matched preferred orientations [3]. At moderate contrast, each edge point activates only a narrow range of orientations (the *active window*), and the window center shifts as the edge normal rotates along the curve. When the total rotation within a half wavelength segment exceeds the window width, no single orientation channel spans the full segment and the representation fragments into short, nearly straight pieces. The inflection point at the center of each segment, where curvature is zero and the tangent is steepest, anchors the perceived straight line.

Together, the two mechanisms produce a zigzag: polarity breaks at peaks and troughs supply the corners, and orientation channel fragmentation straightens the segments.

2 The Model

2.1 V1 orientation tuned edge detectors

Each V1 hypercolumn at retinal position \mathbf{x} contains simple cells tuned to every orientation $\theta \in [0, \pi)$ [7]. Each cell responds primarily to luminance gradients aligned with its preferred direction. The key properties of simple cells relevant to our model are:

- (i) *Oriented linear filtering.* Simple cell receptive fields are well described by Gabor functions [8]. For an odd symmetric (edge detecting) cell, the linear response to a luminance edge is proportional to the projection of the image gradient onto the cell's preferred direction.
- (ii) *Contrast polarity selectivity.* Simple cells are phase sensitive: an odd symmetric cell responds with opposite sign to opposite polarity edges [7]. After rectification, the population encoding a dark to light edge at orientation θ is distinct from the population encoding a light to dark edge at the same orientation. We label these the $+$ and $-$ polarity populations.
- (iii) *Gaussian orientation tuning.* The orientation tuning curve is approximately Gaussian, with a half-width at half-max (HWHM) of $\sim 20^\circ$ [10, 9]. The corresponding Gaussian parameter is $\sigma_\theta = \text{HWHM}/\sqrt{2 \ln 2} \approx 17^\circ \approx 0.30$ rad. This bandwidth is approximately invariant with stimulus contrast [10].
- (iv) *Contrast detection threshold.* Each neuron has a minimum contrast below which it produces no detectable response above its spontaneous firing [7].
- (v) *Divisive normalization.* The contrast response is governed by divisive normalization [6, 4], well described by the Naka–Rushton equation $R(c) = R_{\max} c^n / (\sigma_c^n + c^n)$ with exponent $n \approx 2$ and semi-saturation constant $\sigma_c \approx 0.15$ (Michelson contrast) [4, 1].
- (vi) *Lateral connections.* Long range horizontal connections link neurons at nearby spatial positions whose preferred orientations match the axis connecting them [3]. Psychophysical evidence indicates that contour integration is polarity specific [5], consistent with lateral connections that preferentially link same polarity neurons.

2.2 The linear response at an edge

A *step edge* is a sharp boundary between two regions of different luminance. For instance, the border between a dark line and a lighter background. At every point along such a boundary, two quantities characterize the edge: the *normal direction* θ_n (the direction perpendicular to the boundary, pointing from the darker side to the lighter side), and the *Michelson contrast* $c = (I_{\max} - I_{\min}) / (I_{\max} + I_{\min})$, where I_{\max} and I_{\min} are the luminances on the two sides.

The edge also has a *polarity* $p \in \{+, -\}$, determined by which side is brighter. Consider a neuron whose preferred direction \hat{e}_θ points in the direction of increasing luminance across the edge. Its linear response is positive: the luminance gradient is aligned with the neuron's preferred axis. A neuron whose preferred direction points the opposite way produces a negative linear response of equal magnitude. We call the first neuron a $+$

polarity neuron (for this edge) and the second a – polarity neuron.

Combining the cosine projection (property (i)) with the Gaussian tuning envelope (property (iii)), the linear response of a + polarity neuron tuned to orientation θ at an edge with normal θ_n and contrast c is

$$L(\theta; \theta_n, c) = c \cdot h(\theta - \theta_n), \quad (1)$$

where

$$h(\delta) = \cos \delta \cdot \exp\left(-\frac{\delta^2}{2\sigma_\theta^2}\right) \quad (2)$$

is the *orientation response profile*, with $\delta = \theta - \theta_n$ the angular offset between the neuron's preferred orientation and the edge normal. The profile is the product of the geometric cosine projection and the Gaussian tuning envelope. The response is maximal when $\theta = \theta_n$ (neuron aligned with the gradient) and falls to zero when θ deviates far from θ_n .

A – polarity neuron at the same edge produces the linear response $-L(\theta; \theta_n, c)$: negative, because the luminance gradient opposes its preferred direction. However, V1 simple cells undergo half-wave rectification before their signals are transmitted: the firing rate of a neuron cannot go below its spontaneous baseline, so negative linear responses are clipped to zero [7]. After rectification, only the + polarity population produces a nonzero response to this edge; the – polarity population is silent. At a nearby edge of opposite polarity (e.g., the other side of a line, where the luminance gradient reverses), the roles are exchanged: the – population responds and the + population is silent. This is the physiological basis for the polarity selectivity stated in property (ii).

2.3 Divisive normalization

Following the standard model [6, 4], the firing rate of a neuron tuned to orientation θ (with matching polarity) at an edge with normal θ_n and Michelson contrast c is

$$R(\theta; \theta_n, c) = R_{\max} \frac{[c \cdot h(\theta - \theta_n)]^n}{\sigma_c^n + c^n \mathcal{C}_n}, \quad (3)$$

where the normalization pool energy

$$\mathcal{C}_n = \int_{-\pi/2}^{\pi/2} [h(\varphi)]^n d\varphi \quad (4)$$

sums the n th-power responses across all orientation channels driven by the same edge. With $n = 2$ and $\sigma_\theta \approx 0.30$ rad, numerical integration gives $\mathcal{C}_2 \approx 0.50$.

R_{\max} is a gain parameter; the actual peak firing rate at optimal orientation and high contrast is R_{\max}/\mathcal{C}_n . With $R_{\max} \approx 50$, this gives ~ 100 sp/s, consistent with V1 data [7].

2.4 The active orientation window

A neuron is *active* when $R(\theta) \geq r_{\text{noise}}$, where r_{noise} is the minimum detectable elevation above baseline. Define the relative noise threshold $\rho = r_{\text{noise}}/R_{\max} \approx 0.10$. Substituting (3) into the activity condition and simplifying:

$$h(\theta - \theta_n) \geq \left[\rho \left(\frac{\sigma_c^n}{c^n} + \mathcal{C}_n \right) \right]^{1/n} \equiv \tau_{\text{eff}}(c). \quad (5)$$

Proposition 2.1 (Active orientation window). *At an edge with normal θ_n and Michelson contrast c , a neuron of matching polarity at orientation θ is active if and only if $|\theta - \theta_n| \leq \alpha(c)$, where*

$$h(\alpha(c)) = \tau_{\text{eff}}(c), \quad (6)$$

provided $\tau_{\text{eff}}(c) \leq 1$. If $\tau_{\text{eff}}(c) > 1$, no neuron is active and the edge is invisible. A neuron of the opposite polarity is never active at this edge.

Proof. Since h is strictly decreasing on $[0, \pi/2)$ with $h(0) = 1$ and $h(\pi/2) = 0$, Equation (6) has a unique solution. The neuron is active iff $h(\theta - \theta_n) \geq \tau_{\text{eff}}$, i.e., $|\theta - \theta_n| \leq \alpha$. The opposite-polarity statement follows from rectification. \square

The effective threshold $\tau_{\text{eff}}(c)$ controls how wide the active window is: a lower threshold means more orientations are active. To understand its behavior, note that $\tau_{\text{eff}}(c)$ consists of two terms inside the bracket:

$$\tau_{\text{eff}}(c) = [\rho \sigma_c^n / c^n + \rho \mathcal{C}_n]^{1/n}.$$

The first term, $\rho \sigma_c^n / c^n$, comes from the semi-saturation constant in the normalization denominator: it dominates at low contrast and falls as contrast increases. The second term, $\rho \mathcal{C}_n$, comes from the normalization pool and is independent of contrast: it sets a floor that τ_{eff} can never drop below, no matter how high the contrast. These two terms produce three regimes:

- (i) *Below visibility* ($c < c_{\text{vis}}$). At very low contrast, the first term $\rho \sigma_c^n / c^n$ is large, making $\tau_{\text{eff}} > 1$. Since $h(0) = 1$ is the maximum of h , no orientation satisfies $h(\delta) \geq \tau_{\text{eff}}$, and the edge is invisible. The visibility threshold c_{vis} is the contrast at which $\tau_{\text{eff}} = 1$ exactly, found by setting $\rho(\sigma_c^n / c^n + \mathcal{C}_n) = 1$ and solving for c :

$$c_{\text{vis}} = \sigma_c \left(\frac{\rho}{1 - \rho \mathcal{C}_n} \right)^{1/n} \approx 0.049 \quad (7)$$

($\sim 5\%$ Michelson) with the standard parameters ($\sigma_c = 0.15$, $\rho = 0.10$, $n = 2$, $\mathcal{C}_2 \approx 0.50$). Below this contrast, no V1 neuron fires above its noise floor in response to the edge.

- (ii) *Moderate contrast* (c somewhat above c_{vis}). The first term is still substantial, so τ_{eff} is close to 1 and the active window α is narrow. In this regime, $h(\delta) \approx \cos \delta$ for small δ (the Gaussian factor is nearly flat near $\delta = 0$), and the window half-width is approximately $\alpha \approx \arccos(\tau_{\text{eff}})$. This is the regime in which orientation channel fragmentation is most severe: the window is too narrow to span the tangent variation of a sinusoidal edge.
- (iii) *High contrast* ($c \gg \sigma_c$). The first term $\rho \sigma_c^n / c^n$ becomes negligible, and τ_{eff} approaches the floor set by the second term:

$$\tau_{\infty} = (\rho \mathcal{C}_n)^{1/n} \approx 0.224. \quad (8)$$

The active window therefore approaches

$$\alpha_{\infty} = h^{-1}(\tau_{\infty}) \approx 28^\circ. \quad (9)$$

No matter how high the contrast, the active window cannot exceed $2\alpha_\infty \approx 56^\circ$. This ceiling arises because divisive normalization compresses the peak response: at high contrast, all neurons fire proportionally harder, but the normalization pool grows in step, preventing any neuron from rising far enough above threshold to activate neurons at distant orientations. The Gaussian tuning envelope reinforces this ceiling by ensuring that neurons far from the edge normal produce negligible responses regardless of contrast.

2.5 Lateral connections: orientation and polarity

V1 lateral connections (property (vi)) link neurons at nearby positions with matched preferred orientations and matched contrast polarity [3, 5]. A lateral connection can therefore carry signal between two edge positions \mathbf{x}_1 and \mathbf{x}_2 only if:

- (a) the edges at \mathbf{x}_1 and \mathbf{x}_2 have the *same contrast polarity*; and
- (b) there exists an orientation θ_0 within the active windows at *both* positions.

Condition (a) fails at a polarity reversal: the encoding populations on the two sides of the reversal are entirely disjoint, regardless of orientation. Condition (b) fails when the active windows $[\theta_{n,1} - \alpha, \theta_{n,1} + \alpha]$ and $[\theta_{n,2} - \alpha, \theta_{n,2} + \alpha]$ are disjoint, i.e., when $|\theta_{n,1} - \theta_{n,2}| > 2\alpha$.

The two conditions correspond to the two mechanisms of the model: polarity channel separation (a) and orientation channel fragmentation (b).

3 Curvature Blindness

3.1 The Takahashi stimulus

The standard curvature blindness stimulus consists of a sinusoidal curve $y = A \sin(2\pi x/\lambda)$ drawn against a uniform gray background of luminance I_{bg} . The luminance of the line alternates between $I_{\text{dark}} < I_{\text{bg}}$ and $I_{\text{light}} > I_{\text{bg}}$, with the switch occurring at each peak ($y = A$) and trough ($y = -A$). Each half wavelength segment, from a peak to the next trough or from a trough to the next peak, has a single, uniform contrast polarity against the background.

3.2 Polarity channel separation at peaks and troughs

Proposition 3.1 (Polarity segmentation). *At each peak and trough of the Takahashi stimulus, the contrast polarity reverses. By condition (a) of Section 2.5, lateral connections cannot bridge the polarity boundary. The contour representation is therefore segmented into half wavelength pieces, each encoded by a single polarity neural population.*

Proof. The segment from peak to trough (say) has luminance $I_{\text{dark}} < I_{\text{bg}}$: its edges are encoded by the $-$ polarity population. The next segment (trough to peak) has luminance $I_{\text{light}} > I_{\text{bg}}$: its edges are encoded by the $+$ population. These populations are disjoint (property (ii)), so no lateral connection spans the boundary. \square

Remark 3.2 (Why the illusion requires a gray background). On a *white* background ($I_{\text{bg}} \gg I_{\text{light}} > I_{\text{dark}}$), both line luminances are darker than the background. Both segments therefore have the *same* contrast polarity ($-$) relative to the background. No polarity reversal occurs at peaks and troughs, the lateral chain is unbroken, and the contour is perceived as smooth. On a *black* background, both luminances are lighter than the background, both have polarity $+$, and the same argument applies.

On a *gray* background where $I_{\text{dark}} < I_{\text{bg}} < I_{\text{light}}$, the dark segments have polarity $-$ and the light segments have polarity $+$. The polarity reverses at every peak and trough, the lateral chain is broken, and the segmentation of Proposition 3.1 is in effect. The background dependence of the illusion is thus entirely explained by whether the background luminance falls between or outside the two line luminances.

3.3 Geometry of a half wavelength segment

Each half wavelength segment runs from a peak to the next trough (or vice versa) and has uniform contrast polarity. Within such a segment, the geometry is as follows.

Proposition 3.3 (Half segment geometry). *Consider the segment of $y = A \sin(2\pi x/\lambda)$ from a peak at $x_0 = \lambda/4$ to the next trough at $x_1 = 3\lambda/4$.*

- (i) *The tangent angle $\theta_{\text{tan}}(x) = \arctan(y'(x))$ varies from 0 at the peak to $-\theta_{\text{max}}$ at the midpoint $x_m = \lambda/2$ and back to 0 at the trough, where $\theta_{\text{max}} = \arctan(2\pi A/\lambda)$.*
- (ii) *The midpoint x_m is an inflection point: $y''(x_m) = 0$. Here the curvature is zero and $|\theta_{\text{tan}}|$ is maximal; the curve is locally straightest.*
- (iii) *The edge normal $\theta_n(x) = \theta_{\text{tan}}(x) + \pi/2$ varies within $[\pi/2 - \theta_{\text{max}}, \pi/2]$ over this segment (and symmetrically within $[\pi/2, \pi/2 + \theta_{\text{max}}]$ over the adjacent trough to peak segment).*
- (iv) *The Michelson contrast c between the line and the background is uniform along the segment (single polarity, uniform luminance). Therefore the active window has the same width $2\alpha(c)$ everywhere within the segment.*

Proof. The derivative is $y'(x) = 2\pi A \cos(2\pi x/\lambda)/\lambda$. At $x_0 = \lambda/4$: $\cos(\pi/2) = 0$, so $\theta_{\text{tan}} = 0$. At $x_m = \lambda/2$: $\cos(\pi) = -1$, so $\theta_{\text{tan}} = \arctan(-2\pi A/\lambda) = -\theta_{\text{max}}$. At $x_1 = 3\lambda/4$: $\cos(3\pi/2) = 0$, so $\theta_{\text{tan}} = 0$. The second derivative $y''(x_m) = -(2\pi/\lambda)^2 A \sin(\pi) = 0$ confirms the inflection point. Parts (iii)–(iv) follow directly. \square

3.4 Orientation channel fragmentation within a segment

Proposition 3.4 (Within segment fragmentation). *When $\theta_{\text{max}} > 2\alpha(c)$, the active orientation windows at the endpoints (peak/trough, where $\theta_n = \pi/2$) and at the inflection point (where $\theta_n = \pi/2 - \theta_{\text{max}}$) are disjoint. No single orientation channel spans the full half wavelength segment.*

Proof. The window at the peak is centered at $\pi/2$ with half-width α ; the window at the inflection is centered at $\pi/2 - \theta_{\text{max}}$ with half-width α . These are disjoint when $\theta_{\text{max}} > 2\alpha$.

Every point within the segment remains visible: $\theta_n(x)$ varies continuously, and at each x the orientation $\theta = \theta_n(x)$ lies within the local active window. The gap is in the orientation channel, not in space. \square

3.5 The role of inflection points

Proposition 3.5 (Inflection points anchor straight line perception). *When fragmentation holds ($\theta_{\max} > 2\alpha$), the orientation channel centered near $\theta_0 = \pi/2 - \theta_{\max}$ sees a fragment of the curve surrounding the inflection point. This fragment is the straightest part of the segment: it is centered on the point of zero curvature, and the tangent angle varies by at most 2α across it.*

Proof. The fragment visible at orientation θ_0 consists of positions x where $|\theta_n(x) - \theta_0| \leq \alpha$. At the inflection point x_m , $\theta_n(x_m) = \pi/2 - \theta_{\max}$, which equals θ_0 ; so x_m is in the center of this fragment. The tangent angle within the fragment varies by at most 2α , and since $\kappa(x_m) = 0$ the curve is locally straight at the center of the fragment. \square

Remark 3.6 (Why inflection points are necessary). Inflection points play a specific structural role: they provide the locally straight anchors that the visual system interprets as the “segments” of a zigzag. Without inflection points, for example along a circular arc where curvature never changes sign, fragmentation still breaks the orientation representation into pieces, but every piece is a curved arc of identical shape. There is no locally straight region to anchor a straight segment perception. The model therefore predicts that the illusion requires *sign changing curvature* (i.e., inflection points between successive polarity reversals), not merely polarity switching and moderate contrast.

3.6 The zigzag perception

Proposition 3.7 (Piecewise linear perception). *When both polarity segmentation (Proposition 3.1) and within segment fragmentation (Proposition 3.4) hold, the visual system perceives a zigzag.*

Proof. Polarity segmentation breaks the contour at every peak and trough. Within each half wavelength segment, fragmentation prevents any single orientation channel from tracking the full variation from $\theta_n = \pi/2$ at the endpoints to $\theta_n = \pi/2 - \theta_{\max}$ (or $\pi/2 + \theta_{\max}$ for the adjacent segment) at the inflection. The inflection centered fragment anchors a straight percept (Proposition 3.5). The fragments near the endpoints see a nearly horizontal edge ($\theta_n \approx \pi/2$), consistent with a corner at the peak or trough.

The visual system therefore receives: a polarity break (segment boundary) at each peak and trough, flanked by approximately straight segments passing through the inflection points. The simplest contour consistent with these constraints is a triangular wave i.e a zigzag with corners at the peaks ($y = A$) and troughs ($y = -A$), connected by straight segments with slope $\pm 4A/\lambda$ and corner angle $2 \arctan(4A/\lambda) \approx 8A/\lambda$ for small amplitude. \square

3.7 How curvature and amplitude affect the illusion

Remark 3.8. For large amplitude ($A \sim \lambda$), θ_{\max} is large and the fragmentation condition is easily satisfied, yet the illusion vanishes. The resolution involves the *spatial length* of the fragments that each orientation channel sees.

A neuron tuned to orientation θ_0 sees all curve positions x where $|\theta_n(x) - \theta_0| \leq \alpha$. The edge normal θ_n changes along the curve at a rate determined by the curvature: specifically,

$d\theta_n/ds = \kappa$, where s is arc length and κ is the signed curvature. If κ is approximately constant over the fragment, then the edge normal rotates by $|\kappa| \cdot \Delta s$ over a fragment of arc length Δs . The fragment spans the full active window 2α in orientation, so $|\kappa| \cdot \Delta s \approx 2\alpha$, giving

$$\Delta s \approx \frac{2\alpha}{|\kappa|}. \quad (10)$$

At large amplitude ($A \sim \lambda$), the curvature at the peaks and troughs is large ($|\kappa| \approx (2\pi/\lambda)^2 A$), so each fragment is spatially short. The piecewise-linear approximation then consists of many tiny segments, indistinguishable from a smooth curve at the spatial resolution of the visual system.

However, curvature that is too *small* also undermines the zigzag, for the opposite reason. When $|\kappa|$ is small, Equation (10) gives a long fragment, and the tangent angle varies by the full 2α across it. Although 2α is small in absolute terms (at moderate contrast, $2\alpha \lesssim 56^\circ$), the curvature within the fragment is nonzero, the fragment is an arc, not a line. If the fragment is long enough, this residual curvature is perceptible: the visual system can detect that the fragment bends, even though it cannot compare orientations *across* fragments. The straight segment perception requires fragments that are both long enough to be individually visible and short enough that their internal curvature is below the detection threshold for bending.

The zigzag illusion therefore occupies an intermediate regime: curvature must be high enough that each fragment is short enough to appear straight, but low enough that each fragment is long enough to be perceived as a distinct segment rather than an indistinguishable piece of a smooth curve.

4 Predictions and Limitations

4.1 Predictions

The model yields three necessary conditions and three specific predictions.

Necessary conditions:

The illusion requires: (a) contrast polarity reversals along the curve (to create segment boundaries at peaks/troughs); (b) moderate contrast against the background (to narrow the active orientation window); and (c) inflection points between successive polarity reversals (to anchor straight segment perception within each half wavelength piece).

Predictions:

(i) *Generalization to other curves.* Any polarity alternating curve with sign changing curvature should show the illusion: damped sinusoids, S-curves, and higher order oscillations. Curves without inflection points between polarity switches (arcs of circles or ellipses with polarity alternation) should *not* produce a zigzag percept, though they may appear as disconnected arcs.

(ii) *Contrast window.* Within each half wavelength segment, the fragmentation condition

$\theta_{\max} > 2\alpha(c)$ defines a contrast range $[c_{\text{vis}}, c_{\text{crit}}]$ in which the illusion occurs. The critical contrast c_{crit} depends on A/λ and exists whenever $\theta_{\max} < 2\alpha_{\infty} \approx 56^{\circ}$ ($A/\lambda \lesssim 0.24$).

(iii) *Amplitude dependent contrast window.* The upper critical contrast c_{crit} should increase with A/λ : larger amplitude sinusoids should exhibit the illusion over a wider contrast range.

4.2 Limitations

The model operates at the level of V1 and does not account for curvature selective neurons in V2/V4 that might partially compensate for orientation channel fragmentation.

The claim that lateral connections are polarity specific is supported by the psychophysics of contour integration [5] and by the physiology of horizontal connections [3], but the degree of polarity selectivity in lateral connections has not been measured as precisely as the orientation selectivity. If lateral connections have partial polarity tolerance, the polarity break at peaks/troughs would be leaky rather than absolute, and the illusion strength would degrade gradually rather than switching sharply.

The model uses a single achromatic contrast channel; extending to chromatic contrast (which also produces the illusion [11]) would require replacing the scalar Michelson contrast with a vector-valued color contrast, but the mechanism is unchanged.

The model does not specify the mechanism that converts fragmented orientation representations into a conscious zigzag perception. We have argued that the zigzag is the simplest contour consistent with the available information (polarity breaks at peaks/troughs, approximately straight fragments at inflection points), but a complete model would need to formalize this inference step.

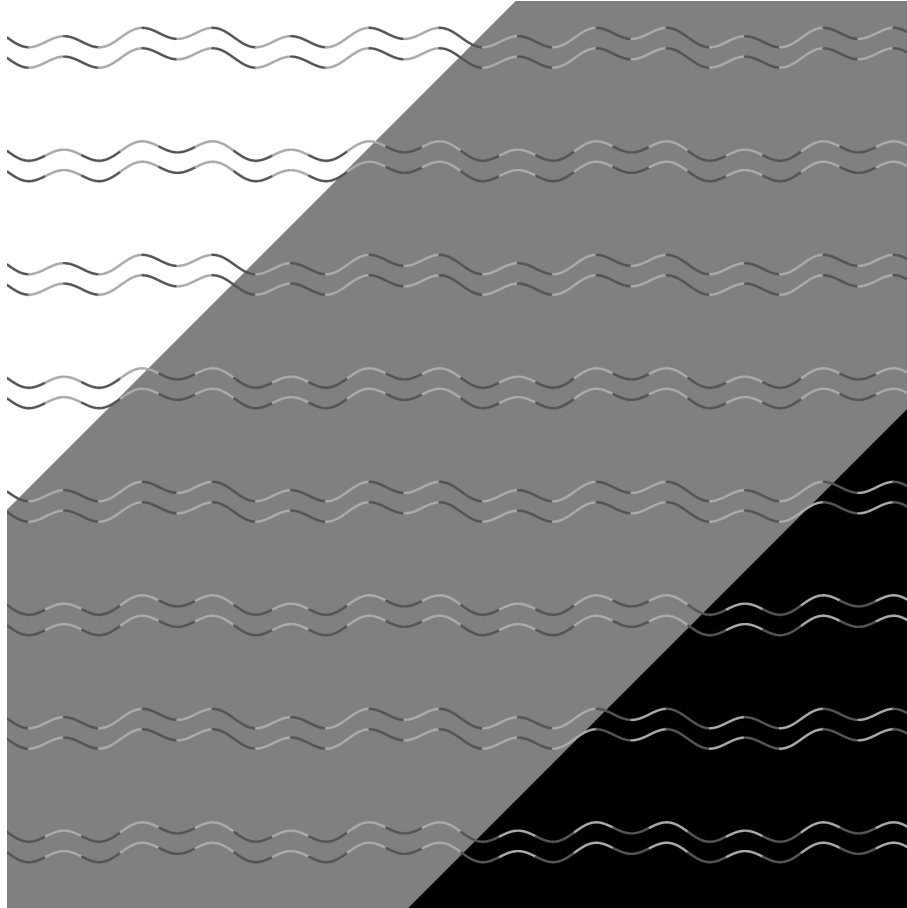


Figure 2: Curvature blindness generalized to a non-sinusoidal curve.

The waveform is $y = 4 \sin(2\pi x/\lambda) + 5 \sin(6\pi x/\lambda)$. The longer segments between extrema still read as curved while the shorter segments are straight. This is consistent with the model as the longer segments have lower average curvature and hence a larger visible window allowing residual curvature to be seen.

References

- [1] D. G. Albrecht and D. B. Hamilton, *Striate cortex of monkey and cat: contrast response function*, J. Neurophysiol. **48**, 217–237 (1982).
- [2] M. Bertamini and A. Kitaoka, *The curvature blindness illusion: is it an illusion of curvature or an illusion of corners?*, i-Perception (2020).
- [3] W. H. Bosking, Y. Zhang, B. Schofield, and D. Fitzpatrick, *Orientation selectivity and the arrangement of horizontal connections in tree shrew striate cortex*, J. Neurosci. **17**, 2112–2127 (1997).
- [4] M. Carandini and D. J. Heeger, *Normalization as a canonical neural computation*, Nat. Rev. Neurosci. **13**, 51–62 (2012).
- [5] D. J. Field, A. Hayes, and R. F. Hess, *Contour integration by the human visual system: evidence for a local “association field”*, Vision Res. **33**, 173–193 (1993).
- [6] D. J. Heeger, *Normalization of cell responses in cat striate cortex*, Vis. Neurosci. **9**, 181–197 (1992).

- [7] D. H. Hubel and T. N. Wiesel, *Receptive fields and functional architecture of monkey striate cortex*, J. Physiol. **195**, 215–243 (1968).
- [8] J. P. Jones and L. A. Palmer, *An evaluation of the two-dimensional Gabor filter model of simple receptive fields in cat striate cortex*, J. Neurophysiol. **58**, 1233–1258 (1987).
- [9] D. L. Ringach, R. M. Shapley, and M. J. Hawken, *Orientation selectivity in macaque V1: diversity and laminar dependence*, J. Neurosci. **22**, 5639–5651 (2002).
- [10] G. Sclar and R. D. Freeman, *Orientation selectivity in the cat's striate cortex is invariant with stimulus contrast*, Exp. Brain Res. **46**, 457–461 (1982).
- [11] K. Takahashi, *Curvature blindness illusion*, i-Perception (2017).